Shahid Bahonar University of Kerman
Journal of Mahani Mathematical Research
Print ISSN: 2251-7952 Online ISSN: 2645-4505
JMMR 2012

ANALYSIS OF DYNAMICS OF FUSION SOLITONS OF THE GENERALIZED (3+1)-KADOMTSEV–PETVIASHVILI EQUATION

M. A. Isah ✉ and A. Yokus

Article type: Research Article

(Received: 08 December 2023, Received in revised form 06 May 2024)

(Accepted: 12 July 2024, Published Online: 13 July 2024)

Abstract. The aim of this paper is to introduce a generalized $(3+1)$-Kadomtsev-Petviashvili equation which is used to describe waves in a ferromagnetic medium. The equation's bilinear form is created and the new homoclinic test approach based on the Hirota bilinear form is used to find numerous novel precise solutions. These accurate solutions, which are depicted in the contour, two-dimensional and three-dimensional graphs, show the evolution of periodic characteristics. The modulation instability is used to investigate the stability of the obtained solutions. Additionally, the development of the fusion soliton is examined, as well as the fusion phenomenon in the traveling wave solution is described in the physical discussion. For this evolution equation, the study indicates new mechanical structures and various characteristics. The derived results back up the model that was proposed. These discoveries open up a new avenue for us to investigate the concept further.

Keywords: The new homoclinic test approach, Stability analysis, Fusion soliton, Kink soliton, Hirota bilinear method.
2020 MSC: Primary 35A08; Secondary 35C07, 35C08, 35Q53.

1. Introduction

Partial differential equations PDEs first appeared in the study of surfaces in geometry [14, 15, 22] and a wide range of problems in mechanics. In the late 19th century, prominent mathematicians from all over the world became actively interested in the study of a broad range of problems caused by partial differential equations [31]. The precise solutions of partial differential equations [21] are necessary to describe complex evolutionary phenomena. Water wave equations or water wave type equations have attracted a lot of attention in the domain of mathematics and physics in recent years [43]. In natural science, there are various nonlinear differential equations which are used to model water wave phenomena [30, 54].

✉ myphysics_09@hotmail.com, ORCID: 0000-0001-9129-5657
https://doi.org/10.22103/jmmr.2024.22632.1547
Publisher: Shahid Bahonar University of Kerman

How to cite: M. A. Isah, A. Yokus, *Analysis of dynamics of fusion solitons of the generalized (3+1)-Kadomtsev–Petviashvili equation*, J. Mahani Math. Res. 2024; 13(2): 505 - 533.

Although all solitary waves have infinite tails, looking for model equations that yield solitary waves with finite spans is truly interesting. Unlike solitons, two such waves would interact for a finite amount of time before becoming completely oblivious to each other. This is equivalent to searching for wavelets with compact support. A compact wave is a powerful solitary wave with compact support that disappears into the background. That is, they all vanish in the same way after they leave a finite core region. In contrast, a compacton is said to be a compact wave that keeps its shape after interacting with another compacton [32, 33]. Compactons are solitary waves with a finite length. Consider

$$u_t + \left(u^a \left(u^b\right)_{xx}\right)_x + \alpha \left(u^m\right)_x = 0. \tag{1}$$

With $a + b \equiv n \geq 1$, and $m \leq a - 1$. Zheng-De and Rosenau [34,53] introduced and explored a family of totally nonlinear KdV equations $n = b = 1, \quad m = 2$ and $m = 3$ to better understand the impact of nonlinear dispersion in the generation of patterns in liquid drops. The well-known Korteweg–de Vries equation is obtained by setting $n = b = 1$ and $m = 2$ as

$$u_t + 6uu_x + u_{xxx} = 0. \tag{2}$$

Here u is the wave amplitude function of the dimensioned space coordinate x and time component t and the subscripts represent the appropriate derivatives, is being used to model wave movement as well as stratified internal waves in fluids, as well as the ion-acoustic wave in plasma. A two-dimensional equation is the Kadomtsev-Petviashvili (KP) equation [3, 12], often called as the two-dimensional KdV equation

$$\left(u_t + 6uu_x + u_{xxx}\right)_x \pm \alpha u_{yy} = 0. \tag{3}$$

Is often used to describe longitudinal waves in a 1-D shallow fluid having short amplitude and gradual dependency mostly on horizontal coordinate, as well as Rayleigh and interior waves in a medium of varying widths and depths [12,38], here $\alpha = +1$ is used when surface tension is smaller than gravitational forces. However, when surface tension is strong, $\alpha = -1$ is chosen. Several methods for getting exact solutions to the non-linear partial differential equation (NLPDE) models have evolved over the past few years, such as the Bernoulli sub-equation function methods [6], the neural network technique [16, 17], the φ^6-model expansion method [13,18,19], the auxiliary equation method [46], the reduction perturbation method [2], the sinh-Gordon function method [47], the improved tanh method [48], the auto-Bäcklund transformation method [25], the generalized exponential rational function method [5], the modified extended tanh-function approach [4], the modified auxiliary equation method [1], the homoclinic technique [49, 50], the symbolic computation method [20], the inverse scattering transformation [7], the variational iteration method [23], the gradient Ricci-Bourguignon soliton [10], the Jacobi elliptic function expansion method [35–37] and so on.

The Kadomtsev-Petviashvili equation is being used to model the nonlinear evolution, small-amplitude long waves in two spatial and one temporal coordinate, gradual dependency on the transverse coordinate. The completely integrable KP model is often used to explain the evolution of quasi-one-dimensional shallow-water waves in a situation where the influences of surface tension and viscosity are negligible [11, 26, 29, 39, 40, 44]. We will look at a generalized $(3+1)$-dimensional Kadomtsev–Petviashvili (GKP) equation in this paper

$$u_{xt} + u_{yt} + \beta(u_x u_y)_x + \alpha u_{yxxx} + \delta u_{zz} = 0. \tag{4}$$

The analytical function u is based on the temporal coordinate t, the propagation distance x, y and z while α, δ, β are arbitrary constants. The fact that equation (4) contains the derivative with respect to the time variable t indicates that the GKP equation is an evolution equation. This indicates that the behaviour or properties of the system can evolve dynamically with time. The Kadomtsev-Petviashvili equation describes weakly dispersive and small-amplitude water waves in the $(3+1)$-dimensional zone in hydrodynamics. This type of equation can be found in almost every major industry [26, 40].

Wang, Li and He et al [11, 40, 44] studied the multi-soliton solutions, Wronskian and Gramian formulations of the model. Wazwaz [39] used the unified form of Hirota's approach to obtain multi-soliton and multi-singular soliton solutions, the multiple exp-function algorithm was used to obtain many soliton solutions by Ma et al [29], Liu et al [27] used the extended homoclinic test method to obtain new exact periodic solitary wave solutions.

This paper's outline can be found below. Section 2 contains an introduction and definition of the Hirota bilinear technique. The new $(3+1)$-Kadomtsev-Petviashvili bilinear transformation is derived in section 3, the Hirota bilinear operation of the equation is then given, which is supported by a theorem. The Hirota bilinear approach is used in section 4 to retrieve new soliton solutions for the GKP model using the homoclinic approach. In the contour, 2D and 3D graphs, the physical aspect of the solitary wave solution is also graphically depicted. Section 5 aims to use the technique of linear stability analysis to assess the stability of the presented equation. Section 6 delves into the physical dynamics of soliton solutions, whereas section 7 delves into the conclusions.

2. Bilinearization technique

Hirota [45] presented a well-known technique for producing numerous solitary wave solutions to fully integrable models named the direct technique. This approach's core idea is to provide new variables into the structure of solutions that are related to the equation's simplified equivalent form via a new variable transformation. Some of the more effective applications of the approach are shown in Ghanbari [8]. Bilinear differential operators were initially presented to the functions (q, p) of a real value x by Hirota

$$D_x (q \cdot p) = \left(\partial_{x_1} - \partial_{x_2}\right) q(x_1)\, p(x_2)\big|_{x_1 = x_2}. \tag{5}$$

We develop the notion to x and t in this expression but usually applied to any set of real parameters, obviously generalizable to any number of real variables for multiple repetitions of the operator and when applying the operator to different values [9, 51]

$$(6)\quad {D_x}^k {D_t}^m (p\cdot q) = (\partial_{x_1} - \partial_{x_2})^k (\partial_{t_1} - \partial_{t_2})^m p(x_1,t_1)\, q(x_2,t_2)\Big|_{x_1=x_2,t_1=t_2}.$$

Where $k, m \geq 0$ and $k+m \geq 1$. Some brief results are offered here to help the D-operator gains some intuition.

$$D_x (p\cdot q) = q p_x - q_x p = -D_x (q.p)\,. \tag{7}$$

$$D_x^2 (p\cdot q) = q p_{xx} - 2 p_x q_x + q_{xx} p. \tag{8}$$

$$D_x D_t (p\cdot q) = p_{xt} q - p_t q_x - p_x q_t + p q_{xt}. \tag{9}$$

Whenever $p = q$

$$D_x^{2n-1} p\cdot p = 0. \tag{10}$$

$$D_x^{2n} p\cdot p = \sum_{k=0}^{2n} (-1)^{2n-k} \binom{2n}{k} \left(\partial_x^k p\right)\left(\partial_x^{2n-k} p\right).$$

On the other hand, bilinear partial derivative forms are related to

$$D_x^k D_t^m (p\cdot p) = \sum_{i=0}^{k}\sum_{j=0}^{m} (-1)^{m+k-j-i} \binom{k}{i}\binom{m}{j} \left(\partial_x^i \partial_t^j p\right)\left(\partial_x^{k-i}\partial_t^{m-j} p\right). \tag{12}$$

For $k, m \geq 1$, as shown [28], this bilinear problem's solution set contains linear subspaces.

3. Bilinear Transformation of The GKP Equation

The bilinear form of equation (4) is the main idea of this section.

A logarithmic transformation known as $p = p(t, y, x, z)$ was developed as an auxiliary function [40]

$$u(t,x,y,z) = \frac{6\alpha}{\beta} (\log p)_x\ . \tag{13}$$

When this equation is applied, certain terms are canceled, which results in having a quadratic equation in variable p, here $p(y, x, z, t)$ is a variational expansion. Here, $\frac{6\alpha}{\beta}$ is the leading constant. When equation (13) is inserted in equation (4), the generalized $(3+1)$-Kadomtsev-Petviashvili model can be expressed as

$$\begin{aligned}(14)\quad 2(pp_{xt} - p_x p_t) + 2\alpha (pp_{xxxy} - p_{xxx}p_y - 3p_{xxy}p_x + 3p_{xx}p_{xy})& \\ +2(pp_{yt} - p_y p_t) + 2\delta\left(pp_{zz} - p_z^2\right) &= 0.\end{aligned}$$

The Hirota bilinear algorithm can be used to linearize the given equation

$$\left[\delta D_z^2 + D_x D_t + D_y D_t + \alpha D_x^3 D_y\right] p.p = 0.$$

Theorem 3.1. *p satisfies equation (13) if and only if* $u(t,x,y,z) = \frac{6\alpha}{\beta}(\log p)_x$ *is a generalized* $(3+1)$*-Kadomtsev-Petviashvili model's solution*

$$\begin{aligned} \left[D_x D_t + \alpha D_x^3 D_y + D_y D_t + \delta D_z^2\right] p.p = {} & 2\left(pp_{xt} - p_x p_t\right) + 2\left(pp_{yt} - p_y p_t\right) \\ & + 2\alpha\left(pp_{xxxy} - p_{xxx}p_y - 3p_{xxy}p_x + 3p_{xx}p_{xy}\right) \\ & + 2\delta\left(pp_{zz} - p_z^2\right) = 0. \end{aligned} \tag{15}$$

4. New Traveling Wave Solutions For GKP Equation

To derive the exact solutions utilizing the Hirota operator in this section, we would use the new homoclinic test technique [3, 52] with an arbitrary constant solution. The function $p(t,y,x,z)$ is assumed to be of the following form

$$p(t,y,x,z) = h_1 e^{\mu} + h_2 e^{-\mu} + h_3 \sinh(\lambda). \tag{16}$$

$$\begin{aligned} \mu &= mx + ny + kz - vt. \\ \lambda &= ax + by + cz - dt. \end{aligned} \tag{17}$$

Here m, k, n, a, b, c, d and v are free variables that are subject to further determination. The following outcomes are generated by putting equations (16), (17) and (13) into equation (3), then gathering the coefficients and equating them to zero

$$\begin{aligned} 8\left(-mv - nv + 4m^3 n\alpha + k^2\delta\right) h_1 h_2 &= 0. \\ 2\begin{pmatrix} d(m+n) + bv - 3a^2 bm\alpha - bm^3\alpha \\ -a^3 n\alpha + a\left(v - 3m^2 n\alpha\right) - 2ck\delta \end{pmatrix} h_1 h_3 &= 0. \\ -2\begin{pmatrix} -(a+b)d - (m+n)v + a^3 b\alpha + 3abm^2\alpha \\ +3a^2 mn\alpha + m^3 n\alpha + \delta\left(c^2 + k^2\right) \end{pmatrix} h_1 h_3 &= 0. \\ -2\begin{pmatrix} d(m+n) + (a+b)v \\ -\left(3a^2 bm + bm^3 + a^3 n + 3am^2 n\right)\alpha - 2ck\delta \end{pmatrix} h_2 h_3 &= 0. \\ -2\begin{pmatrix} -d(a+b) - v(m+n) \\ +\left(a^3 b + 3abm^2 + 3a^2 mn + m^3 n\right)\alpha + \delta\left(c^2 + k^2\right) \end{pmatrix} h_2 h_3 &= 0. \\ 2\left((a+b)d - 4a^3 b\alpha - c^2\delta\right) h_3^2 &= 0. \\ 2\left(-(a+b)d + 4a^3 b\alpha + c^2\delta\right) h_3^2 &= 0. \end{aligned} \tag{18}$$

Using the aforementioned equations, we can arrive at the following results:

Case I:

$$d = \frac{4a^3 b\alpha + c^2\delta}{a+b}, \quad h_1 = 0, \quad h_2 = 0. \tag{19}$$

The exact solution of equation (4) is found using the above case along with equations (13), (16) and (17) as

$$u_1(x,y,z,t) = \frac{6a\alpha \coth\left(ax+by+cz-\left(\frac{4a^3b\alpha+c^2\delta}{a+b}\right)t\right)}{\beta}. \tag{20}$$

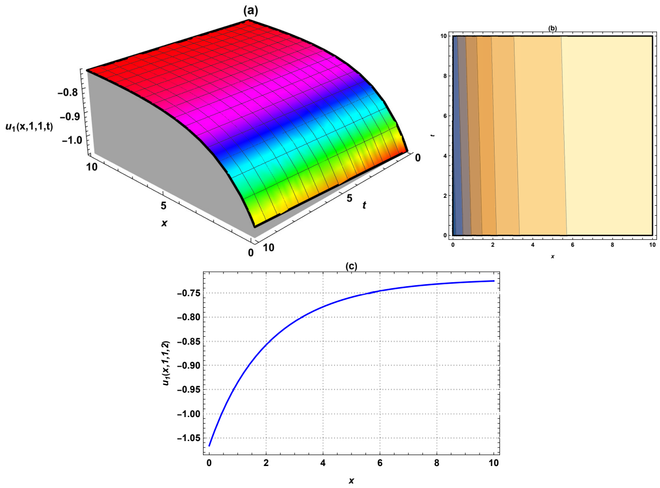

FIGURE 1. The 3D (a), density (b) and 2D (c) graphs of equation (20) for $a = 0.2, b = 0.01, c = 0.8, \beta = -1, \alpha = 0.6, \delta = -0.002, y = 1, z = 1$.

Case 2:

$$b = -a,\ c = \frac{-2a^2\sqrt{\alpha}}{\sqrt{\delta}}, \quad h_1 = 0, \quad h_2 = 0. \tag{21}$$

The exact solution of equation (4) is found using the case 2 along with equations (13), (16) and (17) as

$$u_2(x,y,z,t) = \frac{-6a\alpha}{\beta} \coth\left(dt + a\left(-x+y+\frac{2az\sqrt{\alpha}}{\sqrt{\delta}}\right)\right). \tag{22}$$

Case 3:

$$h_3 = 0,\ v = \frac{4m^3n\alpha + k^2\delta}{m+n}. \tag{23}$$

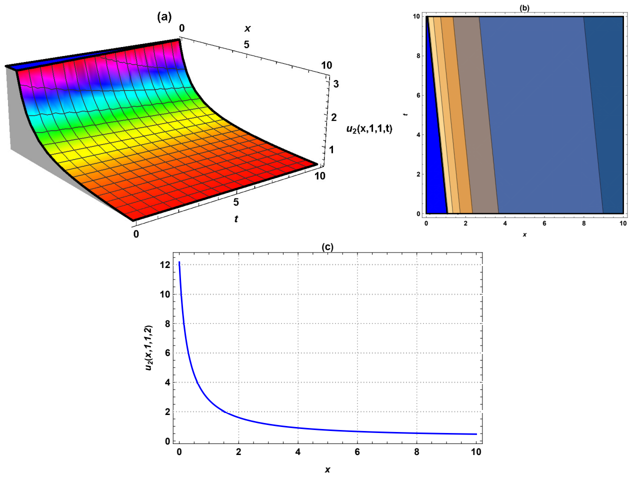

FIGURE 2. The 3D (a), density (b) and 2D (c) graphs of equation (22) for $n = 7.8, h_1 = 0.3, h_2 = 8.4, k = 4.2, \beta = 0.45, \delta = 1.8, \alpha = 0.3, y = 1, z = 1, m = 0.5$

The kink soliton solution of equation (4) is found using the above case along with equations (13), (16) and (17) as

(24)
$$u_3(x,y,z,t) = \frac{6\alpha m\left(h_1 e^{mx+ny+kz-\left(\frac{4m^3n\alpha+k^2\delta}{m+n}\right)t} - h_2 e^{-mx-ny-kz+\left(\frac{4m^3n\alpha+k^2\delta}{m+n}\right)t}\right)}{\beta\left(h_1 e^{mx+ny+kz-\left(\frac{4m^3n\alpha+k^2\delta}{m+n}\right)t} + h_2 e^{-mx-ny-kz+\left(\frac{4m^3n\alpha+k^2\delta}{m+n}\right)t}\right)}.$$

Case 4:

(25)
$$k = \frac{-2m^2\sqrt{\alpha}}{\sqrt{\delta}}, \quad h_3 = 0, \;\; n = -m.$$

The exact solution of equation (4) is obtained using the above case together with equations (13), (16) and (17) as

(26)
$$u_4(x,y,z,t) = \frac{6\alpha m\left(h_1 e^{2mx} - h_2 e^{2tv+2m\left(y+\frac{2mz\sqrt{\alpha}}{\sqrt{\delta}}\right)}\right)}{\beta\left(h_1 e^{2mx} + h_2 e^{2tv+2m\left(y+\frac{2mz\sqrt{\alpha}}{\sqrt{\delta}}\right)}\right)}.$$

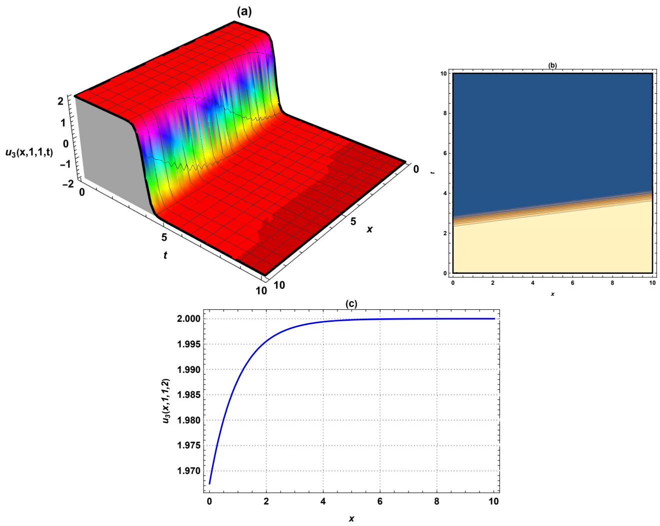

FIGURE 3. The 3D (a), density (b) and 2D (c) graphs of equation (24) for $m = 0.5, n = 7.8, h_1 = 0.3, h_2 = 8.4, k = 4.2, \beta = 0.45, \delta = 1.8, \alpha = 0.3, y = 1, z = 1$.

Case 5:

$$\delta = \frac{v\,(m+n) - 4m^3 n\alpha}{k^2}, \quad h_3 = 0, \; n = n. \tag{27}$$

The exact solution of equation (4) is found using the above case along with Equations(13), (16) and (17) as

$$u_5(x, y, z, t) = \frac{6\alpha m \left(h_1 e^{2(mx+ny+kz)} - h_2 e^{2tv}\right)}{\beta \left(h_1 e^{2(mx+ny+kz)} + h_2 e^{2tv}\right)}. \tag{28}$$

Case 6:

$$\delta = \frac{d\,(a+b) - 4a^3 b\alpha}{c^2}, \; h_1 = 0, \; h_2 = 0, \; n = n. \tag{29}$$

The exact solution of equation (4) is derived by using the case (6) together with equations(13), (16) and (17) as

$$u_6(x, y, z, t) = \frac{-6a\alpha}{\beta} \coth\left(dt - ax - by - cz\right). \tag{30}$$

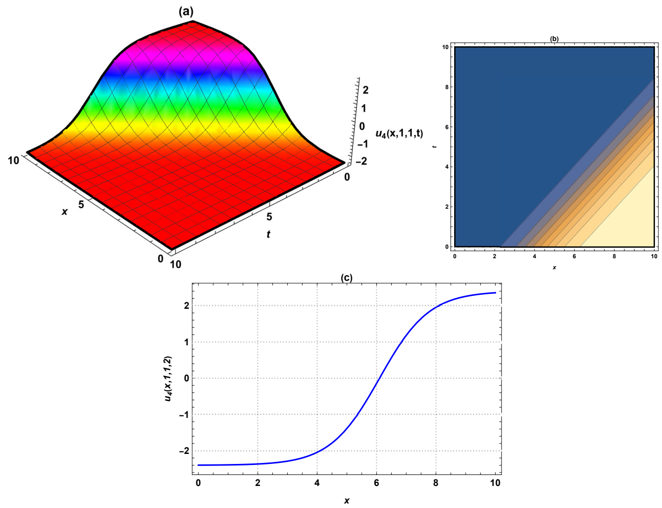

FIGURE 4. The 3D (a), density (b) and 2D (c) graphs of equation (26) for $m = 0.6, v = 0.55, h_1 = 0.3, h_2 = 8.4, \beta = 0.45, \delta = 1.8, \alpha = 0.3, y = 1, z = 1$.

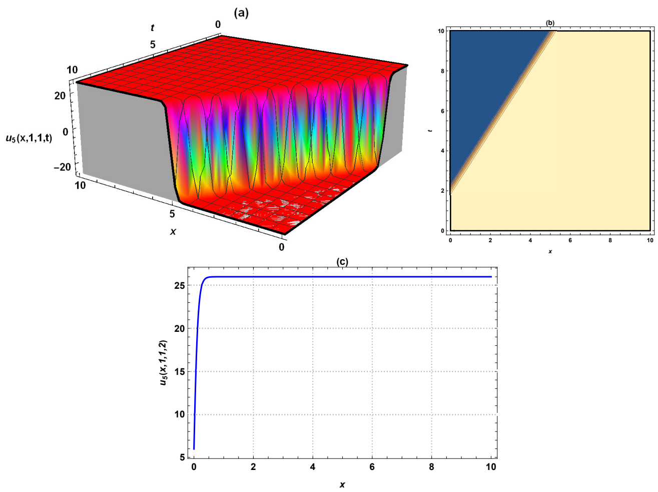

FIGURE 5. The 3D (a), density (b) and 2D (c) graphs of equation (28) for $n = 0.8, v = 4.2, h_1 = 0.3, m = 6.5, h_2 = 8.4, k = 9.5, \beta = 0.45, \alpha = 0.3, y = 1, z = 1$.

Case 7:

$$m = \frac{\sqrt{-ab\,(a-3b)}}{\sqrt{a+b}},\ v = \frac{-bd\sqrt{a+b}\,(a-3b)^3}{4\,(-ab\,(a-3b))^{\frac{3}{2}}},$$

$$\delta = 0,\ n = \frac{ab\sqrt{a+b}}{\sqrt{-ab\,(a-3b)}},\qquad \alpha = \frac{(a+b)\,d}{4a^3b}. \tag{31}$$

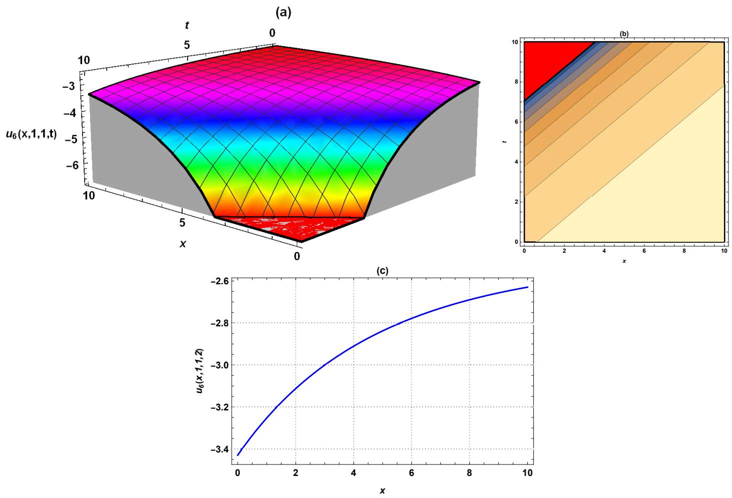

FIGURE 6. The 3D (a), density (b) and 2D (c) surfaces of equation(30) for $a = 0.09, b = 0.06, c = 1.08, h_1 = 0.3, h_2 = 8.4, d = 0.108, \beta = 0.45, \alpha = -2.08, y = 1, z = 1$.

The exact solution of equation (4) is found using the above case along with equations (13), (16) and (17).

$$u_7(x,y,z,t) = \frac{3d\,(a+b)\left(\begin{array}{l} \dfrac{\sqrt{-a(a-3b)b}\,\mathrm{e}^{\frac{(a-3b)^3 b\sqrt{a+b}dt}{4(-a(a-3b)b)^{3/2}}+\frac{\sqrt{-a(a-3b)b}x}{\sqrt{a+b}}+\frac{ab\sqrt{a+b}y}{\sqrt{-a(a-3b)b}}+kz}h_1}{\sqrt{a+b}} \\ -\dfrac{\sqrt{-a(a-3b)b}\,\mathrm{e}^{-\frac{(a-3b)^3 b\sqrt{a+b}dt}{4(-a(a-3b)b)^{3/2}}-\frac{\sqrt{-a(a-3b)b}x}{\sqrt{a+b}}-\frac{ab\sqrt{a+b}y}{\sqrt{-a(a-3b)b}}-kz}h_2}{\sqrt{a+b}} \\ +a\cosh\left[dt-ax-by-cz\right]h_3 \end{array}\right)}{2a^2b\beta\left(\begin{array}{l} \mathrm{e}^{\frac{(a-3b)^3 b\sqrt{a+b}dt}{4(-a(a-3b)b)^{3/2}}+\frac{\sqrt{-a(a-3b)b}x}{\sqrt{a+b}}+\frac{ab\sqrt{a+b}y}{\sqrt{-a(a-3b)b}}+kz}h_1 \\ +\mathrm{e}^{-\frac{(a-3b)^3 b\sqrt{a+b}dt}{4(-a(a-3b)b)^{3/2}}-\frac{\sqrt{-a(a-3b)b}x}{\sqrt{a+b}}-\frac{ab\sqrt{a+b}y}{\sqrt{-a(a-3b)b}}-kz}h_2 \\ -\sinh\left[dt-ax-by-cz\right]h_3 \end{array}\right)}. \tag{32}$$

Case 8:

$$m = -a, \quad n = -b, \; v = -d, \; \alpha = \frac{d\,(a+b)}{4a^3b}, \; \delta = 0. \tag{33}$$

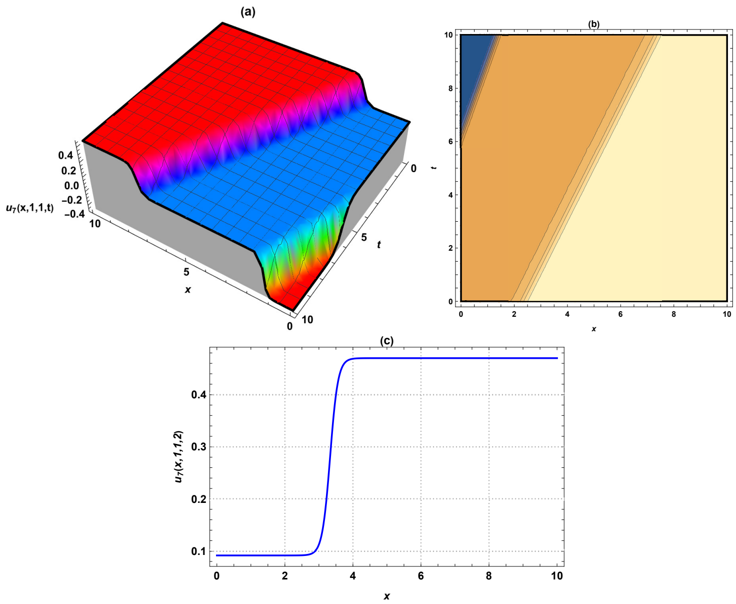

FIGURE 7. The 3D (a), density (b) and 2D (c) surfaces of equation (32) for $a = 2.08, b = 20.8, c = 2.3, k = 0.03, h_1 = 0.3, h_2 = 0.4, h_3 = 1.6, d = 0.108, \beta = 0.45, y = 1, z = 1$.

The exact solution of equation (4) is retrived by using the case above together with equations (13), (16) and (17) as

(34)
$$u_8(x,y,z,t) = \frac{-3d\,(a+b)\begin{pmatrix} h_1 e^{2dt+2kz} - h_2 e^{2ax+2by} \\ -h_3 e^{dt+ax+by+kz}\cosh\left(dt-ax-by-cz\right)\end{pmatrix}}{2a^2 b\beta\begin{pmatrix} h_1 e^{2dt+2kz} + h_2 e^{2ax+2by} \\ -h_3 e^{dt+ax+by+kz}\sinh\left(dt-ax-by-cz\right)\end{pmatrix}}.$$

Case 9:

(35)
$$m = a, \quad n = b, \;\; v = d, \;\; \alpha = \frac{d\,(a+b)}{4a^3 b}, \;\; \delta = 0.$$

The exact solution of equation (4) is retrieved by using the case above, along with equations(13), (16) and (17) as

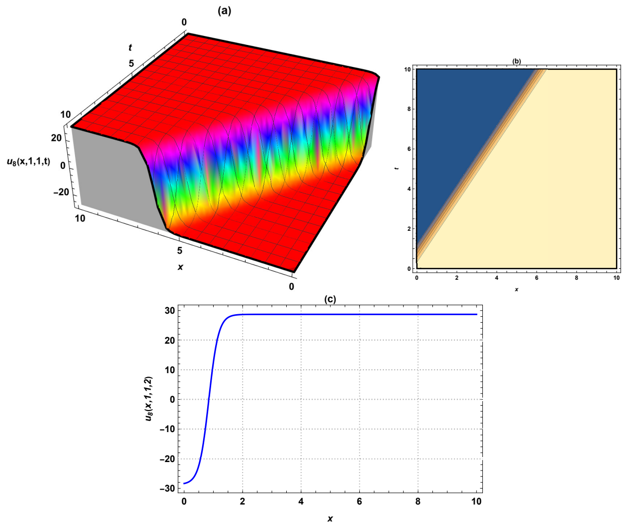

FIGURE 8. The 3D (a), density (b) and 2D (c) graphs of equation (34) for $a = 3.02, b = 0.08, c = 1.3, d = 2.028, k = 0.3, h_1 = 0.3, h_2 = 0.4, h_3 = 1.6, \beta = 0.45, y = 1, z = 1$.

(36)
$$u_9(x,y,z,t) = \frac{3d\,(a+b)\begin{pmatrix} h_1 e^{2(ax+by+kz)} - h_2 e^{2dt} \\ +h_3 e^{dt+ax+by+kz}\cosh\left(dt-ax-by-cz\right)\end{pmatrix}}{2a^2 b\beta\begin{pmatrix} h_1 e^{2(ax+by+kz)} + h_2 e^{2dt} \\ -h_3 e^{dt+ax+by+kz}\sinh\left(dt-ax-by-cz\right)\end{pmatrix}}.$$

Case 10:

$$a = 0,\ b = 0,\ c = 0,\ h_2 = 0,\quad m = \frac{-i\delta^{\frac{1}{4}}\sqrt{k}}{\alpha^{\frac{1}{4}}},\quad n = \frac{i\delta^{\frac{1}{4}}\sqrt{k}}{\alpha^{\frac{1}{4}}}. \tag{37}$$

The exact solution of equation (4) is retrieved by using the case 10, along with equations(13), (16) and (17) as

$$u_{10}(x,y,z,t) = \frac{-6ih_1\alpha^{\frac{3}{4}}\delta^{\frac{1}{4}}\sqrt{k}e^{\left(kz+\frac{iy\delta^{\frac{1}{4}}\sqrt{k}}{\alpha^{\frac{1}{4}}}\right)}}{\left(h_1\beta e^{\left(kz+\frac{iy\delta^{\frac{1}{4}}\sqrt{k}}{\alpha^{\frac{1}{4}}}\right)} - h_3\beta e^{\left(tv+\frac{ix\delta^{\frac{1}{4}}\sqrt{k}}{\alpha^{\frac{1}{4}}}\right)}\sinh\left(dt\right)\right)}. \tag{38}$$

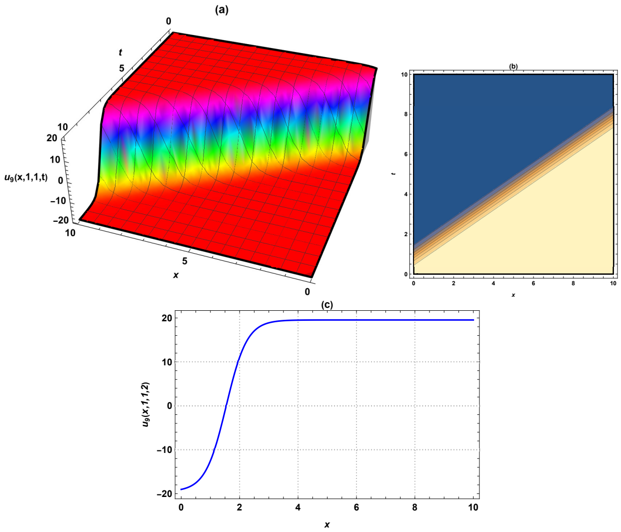

FIGURE 9. The 3D (a), density (b) and 2D (c) graphs of equation(36) for $a = 1.4, b = 0.3, c = 2.8, d = 2.028, k = -0.4, h_1 = 0.3, h_2 = 0.4, h_3 = 1.6, \beta = 0.45, y = 1, z = 1$.

Case 11:

$$a = 0,\ b = 0,\ c = 0,\ h_2 = 0,\quad m = \frac{-\delta^{\frac{1}{4}}\sqrt{k}}{\alpha^{\frac{1}{4}}},\quad n = \frac{\delta^{\frac{1}{4}}\sqrt{k}}{\alpha^{\frac{1}{4}}}. \tag{39}$$

The exact solution of equation (4) is found using the above case along with equations (13), (16) and (17) as

$$u_{11}(x,y,z,t) = \frac{-6h_1\alpha^{\frac{3}{4}}\delta^{\frac{1}{4}}\sqrt{k}e^{\left(kz+\frac{y\delta^{\frac{1}{4}}\sqrt{k}}{\alpha^{\frac{1}{4}}}\right)}}{h_1\beta e^{\left(kz+\frac{y\delta^{\frac{1}{4}}\sqrt{k}}{\alpha^{\frac{1}{4}}}\right)} - h_3\beta e^{\left(tv+\frac{x\delta^{\frac{1}{4}}\sqrt{k}}{\alpha^{\frac{1}{4}}}\right)}\sinh(dt)}. \tag{40}$$

Case 12:

$$\begin{aligned} a &= 0,\ h_2 = 0,\quad m = \frac{-\delta^{\frac{1}{4}}\sqrt{k}}{\alpha^{\frac{1}{4}}},\quad n = \frac{\delta^{\frac{1}{4}}\sqrt{k}}{\alpha^{\frac{1}{4}}}, \\ d &= \frac{c^2\delta}{b},\quad v = \frac{-b\alpha^{\frac{1}{4}}\delta^{\frac{3}{4}}k^{\frac{3}{2}} + 2ck\delta}{b}. \end{aligned} \tag{41}$$

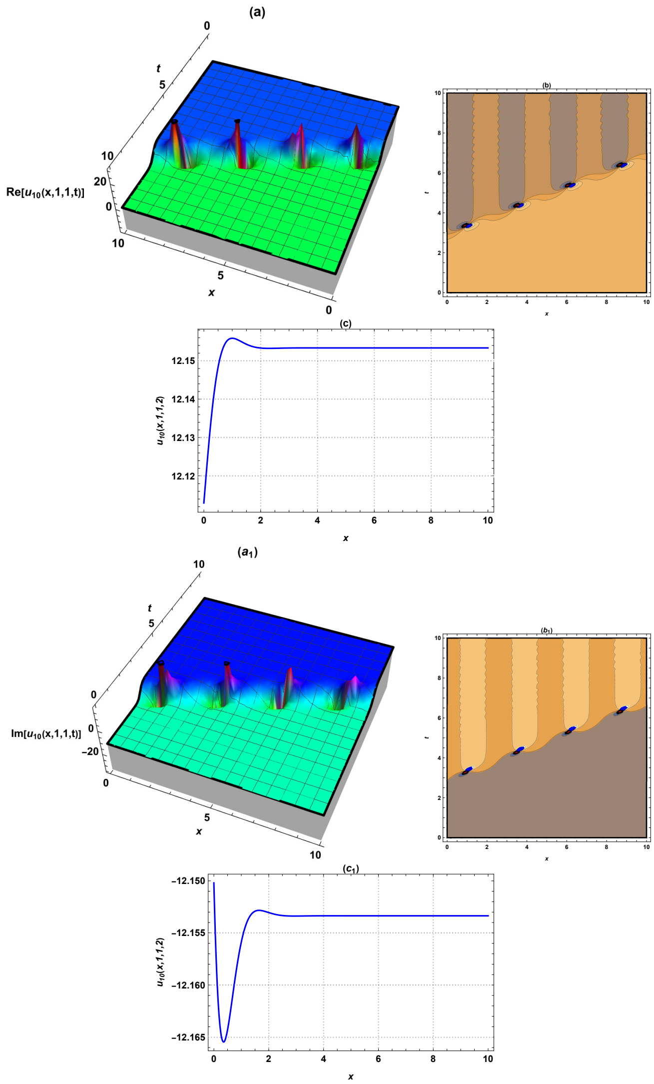

FIGURE 10. The 3Ds (a), (a_1), densities (b), (b_1) and 2Ds (c), (c_1) surfaces of equation(38) for $v = 4.2, \alpha = 2.04, \delta = -0.8, d = 2.028, k = 18.9, h_1 = 2.3, h_3 = 0.6, \beta = 0.45, y = 1, z = 1$.

The exact solution of equation (4) is found using the case (12) along with equations (13), (16) and (17) as
(42)

$$u_{12}(x,y,z,t) = \frac{-6h_1\alpha^{\frac{3}{4}}\delta^{\frac{1}{4}}\sqrt{k}e^{\left(kz+\frac{y\delta^{\frac{1}{4}}\sqrt{k}}{\alpha^{\frac{1}{4}}}\right)}}{\left(\begin{array}{c} h_1\beta e^{\left(kz+\frac{y\delta^{\frac{1}{4}}\sqrt{k}}{\alpha^{\frac{1}{4}}}\right)} \\ +h_3\beta e^{\left(\frac{x\delta^{\frac{1}{4}}\sqrt{k}}{\alpha^{\frac{1}{4}}}-k^{\frac{3}{2}}t\alpha^{\frac{1}{4}}\delta^{\frac{3}{4}}+\frac{2ckt\delta}{b}\right)}\sinh\left(by+cz-\frac{c^2\delta}{b}t\right)\end{array}\right)}.$$

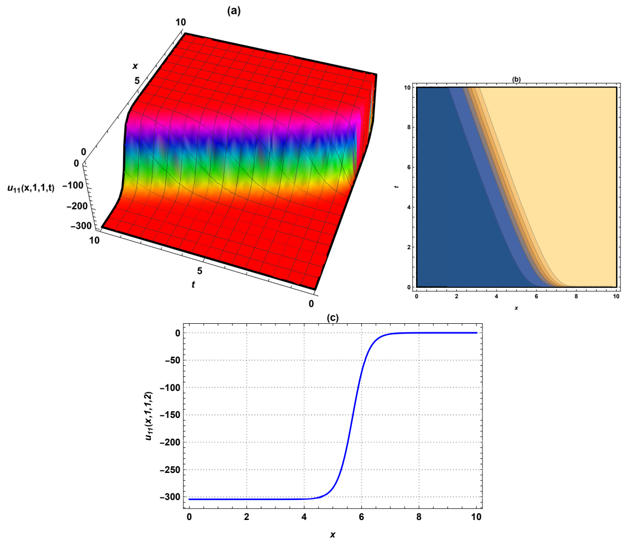

FIGURE 11. The 3D (a), density (b) and 2D (c) surfaces of equation(40) for $d = 0.08, k = 18.02, v = 1.2, h_1 = -0.8, h_3 = 0.6, \beta = 0.45, \alpha = 6.04, \delta = 3.8, y = 1, z = 1$.

Case 13:

$$\begin{aligned} a &= 0,\ n = 0, \quad c = \frac{bm^2\sqrt{\alpha} + bk\sqrt{\delta}}{m\sqrt{\delta}}, \\ d &= bm^2\alpha + 2bk\sqrt{\alpha}\sqrt{\delta} + \frac{bk^2\delta}{m^2}, \quad v = \frac{k^2\delta}{m}. \end{aligned} \tag{43}$$

The soliton solution of equation (4) is retrieved by using the case above, together with equations(13), (16) and (17) as

(44)

$$u_{13}(x,y,z,t) = \frac{6m\alpha\left(h_1 e^{2mx+2kz} - h_2 e^{\frac{2tk^2\delta}{m}}\right)}{\beta\left(\begin{array}{c} h_1 e^{2mx+2kz} + h_2 e^{\frac{2tk^2\delta}{m}} \\ +h_3 e^{mx+kz+\frac{tk^2\delta}{m}} \sinh\left(b\left(y - \frac{\left(m^2\sqrt{\alpha}+k\sqrt{\delta}\right)\left(-mz+m^2t\sqrt{\alpha}\sqrt{\delta}+kt\delta\right)}{m^2\sqrt{\delta}}\right)\right)\end{array}\right)}.$$

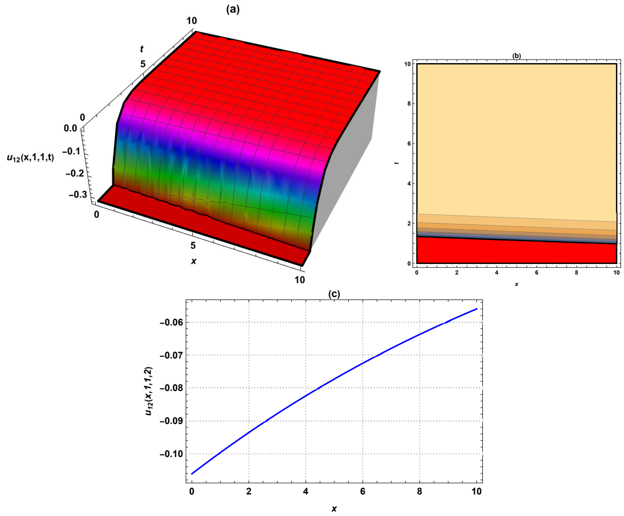

FIGURE 12. The 3D (a), density (b) and 2D (c) graphs of equation (42) for $a = -0.5, c = 0.3, k = 0.0021, h_1 = 0.82, h_3 = 0.8, \beta = 0.6, \alpha = 2.04, \delta = 9.8, y = 1, z = 1$.

Case 14:

(45)
$$\begin{aligned} a &= a,\ b=0,\ m=0,\ \ c=\frac{na^2\sqrt{\alpha}+ak\sqrt{\delta}}{n\sqrt{\delta}}, \\ d &= \frac{a^3n^2\alpha+2a^2kn\sqrt{\alpha}\sqrt{\delta}+ak^2\delta}{n^2},\quad v=\frac{k^2\delta}{n}. \end{aligned}$$

The exact solution of equation (4) is obtained by using the case above together with equations(13), (16) and (17) as

(46)
$$u_{14}(x,y,z,t)=\frac{6ah_3\alpha e^{ny+kz+\frac{k^2\delta t}{n}}\cosh\left(a\left(x-a^2t\alpha+\frac{a\sqrt{\alpha}(nz-2kt\delta)}{n\sqrt{\delta}}+\frac{k(nz-kt\delta)}{n^2}\right)\right)}{\beta\left(\begin{array}{c} h_1e^{2ny+2kz}+h_2e^{\frac{2tk^2\delta}{n}} \\ +h_3e^{ny+kz+\frac{tk^2\delta}{n}}\sinh\left(a\left(x-a^2t\alpha+\frac{a\sqrt{\alpha}(nz-2kt\delta)}{n\sqrt{\delta}}+\frac{k(nz-kt\delta)}{n^2}\right)\right)\end{array}\right)}.$$

Case 15:

(47)
$$\begin{aligned} a &= \frac{-i\delta^{\frac{1}{4}}\sqrt{k}}{\sqrt{2}\alpha^{\frac{1}{4}}},\ b=\frac{i\delta^{\frac{1}{4}}\sqrt{k}}{\sqrt{2}\alpha^{\frac{1}{4}}},\ m=\frac{-i\delta^{\frac{1}{4}}\sqrt{k}}{\sqrt{2}\alpha^{\frac{1}{4}}}, \\ c &= k,\ \ n=\frac{i\delta^{\frac{1}{4}}\sqrt{k}}{\sqrt{2}\alpha^{\frac{1}{4}}}. \end{aligned}$$

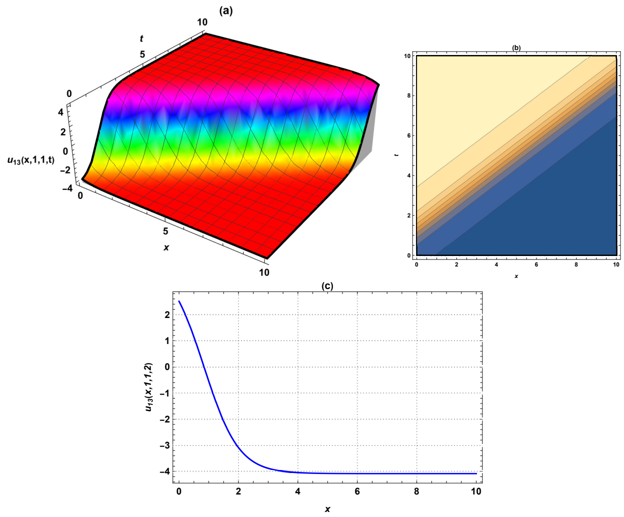

FIGURE 13. The 3D (a), density (b) and 2D (c) graphs of equation(44) for $b = 0.008, m = 0.85, k = 0.5, h_1 = 3.08, h_2 = 0.4, h_3 = 0.06, \beta = -3.8, \alpha = 3.04, \delta = 3.8, y = 1, z = 1$.

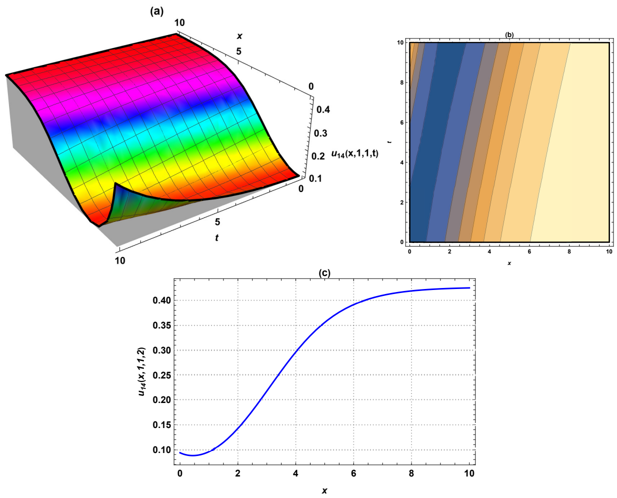

FIGURE 14. The 3D (a), density (b) and 2D (c) surfaces of equation(46) for $a = 0.8, n = 0.8, k = 0.12, h_1 = 0.8, h_2 = 2.4, h_3 = 0.6, \beta = 0.45, \alpha = 0.04, \delta = 3.8, y = 1, z = 1$.

The exact solution of equation (4) is found using the above case along with equations(13), (16) and (17) as
(48)

$$u_{15}(x,y,z,t) = \frac{-3i\sqrt{2}\sqrt{k}\alpha^{\frac{3}{4}}\delta^{\frac{1}{4}}\left(\begin{array}{c} h_1 e^{2kz+\frac{iy\delta^{\frac{1}{4}}\sqrt{2k}}{\alpha^{\frac{1}{4}}}} - h_2 e^{2tv+\frac{ix\delta^{\frac{1}{4}}\sqrt{2k}}{\alpha^{\frac{1}{4}}}} \\ +h_3 e^{tv+kz+\frac{i(x+y)\delta^{\frac{1}{4}}\sqrt{k}}{\sqrt{2}\alpha^{\frac{1}{4}}}}\cosh\left(dt-kz+\frac{i(x-y)\delta^{\frac{1}{4}}\sqrt{k}}{\sqrt{2}\alpha^{\frac{1}{4}}}\right)\end{array}\right)}{\beta\left(\begin{array}{c} h_1 e^{2kz+\frac{iy\delta^{\frac{1}{4}}\sqrt{2k}}{\alpha^{\frac{1}{4}}}} + h_2 e^{2tv+\frac{ix\delta^{\frac{1}{4}}\sqrt{2k}}{\alpha^{\frac{1}{4}}}} \\ -h_3 e^{tv+kz+\frac{i(x+y)\delta^{\frac{1}{4}}\sqrt{k}}{\sqrt{2}\alpha^{\frac{1}{4}}}}\sinh\left(dt-kz+\frac{i(x-y)\delta^{\frac{1}{4}}\sqrt{k}}{\sqrt{2}\alpha^{\frac{1}{4}}}\right)\end{array}\right)}.$$

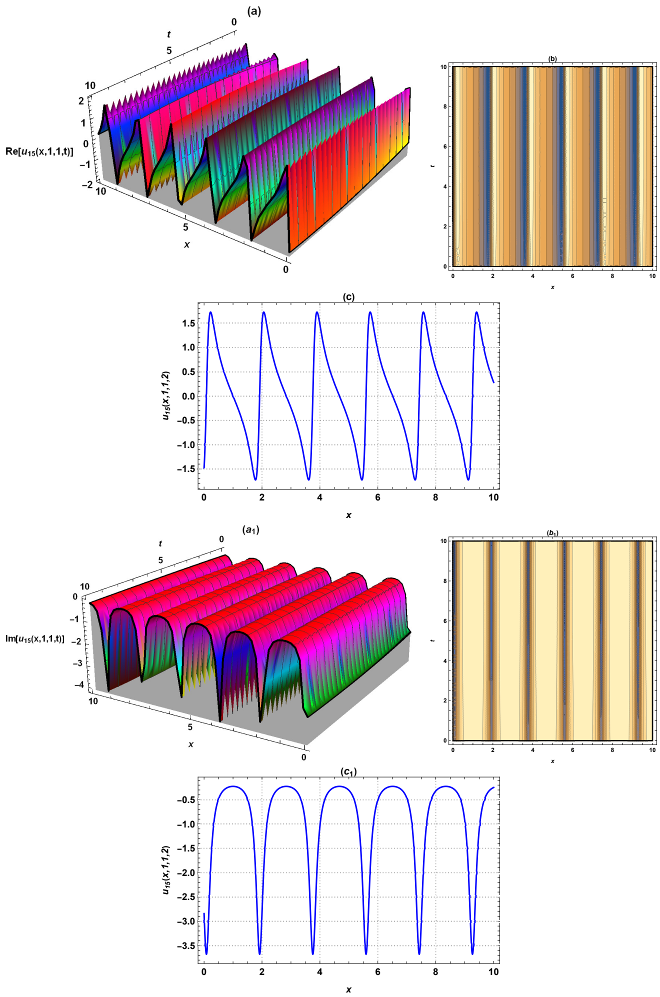

FIGURE 15. The 3Ds (a), (a_1), densities (b),(b_1) and 2Ds (c),(c_1) surfaces of equation(48) for $d = -0.08, v = 0.02, k = 0.6, h_1 = 0.8, h_2 = 2.4, h_3 = 0.6, \beta = 0.45, \alpha = 0.04, \delta = 3.8, y = 1, z = 1$.

Case 16:

$$a = \frac{-\delta^{\frac{1}{4}}\sqrt{k}}{\sqrt{2}\alpha^{\frac{1}{4}}},\ b = \frac{\delta^{\frac{1}{4}}\sqrt{k}}{\sqrt{2}\alpha^{\frac{1}{4}}},\ m = \frac{\delta^{\frac{1}{4}}\sqrt{k}}{\sqrt{2}\alpha^{\frac{1}{4}}}, \qquad (49)$$
$$c = -k,\ \ n = \frac{-\delta^{\frac{1}{4}}\sqrt{k}}{\sqrt{2}\alpha^{\frac{1}{4}}}.$$

The exact solution of equation (4) is obtained using the above case together with equations(13), (16) and (17) as

(50)
$$u_{16}(x,y,z,t) = \frac{3\sqrt{2}\sqrt{k}\alpha^{\frac{3}{4}}\delta^{\frac{1}{4}}\left(\begin{array}{c} h_1 e^{2kz+\frac{x\delta^{\frac{1}{4}}\sqrt{2k}}{\alpha^{\frac{1}{4}}}} - h_2 e^{2tv+\frac{y\delta^{\frac{1}{4}}\sqrt{2k}}{\alpha^{\frac{1}{4}}}} \\ -h_3 e^{tv+kz+\frac{(x+y)\delta^{\frac{1}{4}}\sqrt{k}}{\sqrt{2}\alpha^{\frac{1}{4}}}}\cosh\left(dt+kz+\frac{(x-y)\delta^{\frac{1}{4}}\sqrt{k}}{\sqrt{2}\alpha^{\frac{1}{4}}}\right)\end{array}\right)}{\beta\left(\begin{array}{c} h_1 e^{2kz+\frac{x\delta^{\frac{1}{4}}\sqrt{2k}}{\alpha^{\frac{1}{4}}}} + h_2 e^{2tv+\frac{y\delta^{\frac{1}{4}}\sqrt{2k}}{\alpha^{\frac{1}{4}}}} \\ -h_3 e^{tv+kz+\frac{(x+y)\delta^{\frac{1}{4}}\sqrt{k}}{\sqrt{2}\alpha^{\frac{1}{4}}}}\sinh\left(dt+kz+\frac{(x-y)\delta^{\frac{1}{4}}\sqrt{k}}{\sqrt{2}\alpha^{\frac{1}{4}}}\right)\end{array}\right)}.$$

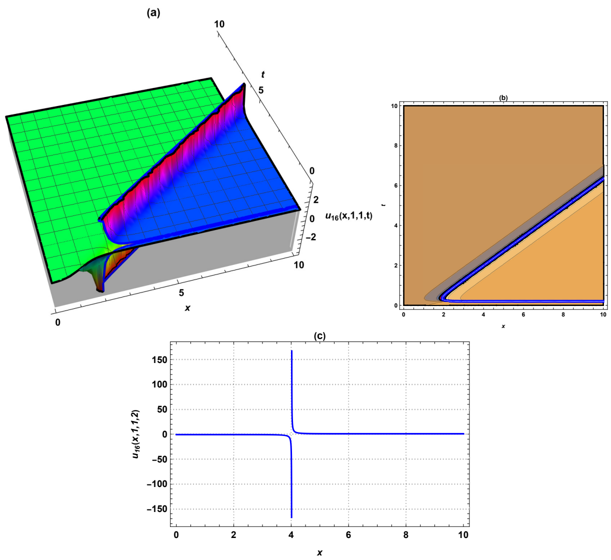

FIGURE 16. The 3D (a), density (b) and 2D (c) surfaces of equation (50) for $d = 0.08, v = 4.8, k = 0.6, h_1 = 0.8, h_2 = 2.4, h_3 = 0.6, \beta = 0.45, \alpha = 0.04, \delta = 3.8, y = 1, z = 1$.

5. Analysis of the GKP Equation's Stability

In this part, the linear stability analysis technique [41] will be utilized to assess the stability of the proposed equation (4). Considering the perturbed solution of the form

$$u\left(t,y,x,z\right)=r+\lambda v\left(t,y,x,z\right). \tag{51}$$

A steady state solution of equation (4) can easily be shown for any constant r. When equation (51) is substituted in equation (4) the result is

$$\beta\lambda^2 v_{tx}v_y+\beta\lambda^2 v_t v_{xy}+\alpha\lambda v_{yxxx}+\delta\lambda v_{zz}+\lambda v_{xt}+\lambda v_{yt}=0. \tag{52}$$

Linearizing the above equation in λ

$$\alpha v_{yxxx}+\delta v_{zz}+v_{xt}+v_{yt}=0. \tag{53}$$

Assuming the above equation (53) has a solution in the form of

$$v\left(x,y,z,t\right)=e^{i(Lx+My+Nz-\mu t)}. \tag{54}$$

Here L, M and N are normalized wave numbers, one can get the following by inserting equation (54) into equation (53)

$$\mu\left(L,M,N\right)=\frac{\delta N^2-\alpha L^3 M}{L+M}. \tag{55}$$

The propagation relationships in equation (55) are studied. The $\mu(L,N,M)$'s sign implies that the solution will grow or shrink in size as time goes by. The dispersion relation equation (55)'s steady-state stability is assessed via stimulated Raman scattering, self-phase modulation along with group velocity dispersion. When $\mu(L,M,N)\neq 0$, the wave numbers N, L and M are real and the steady-state is stable even when changed slightly, whilst $\mu(L,N,M)=0$, at this point, the steady-state solution happens to be unstable, the wave numbers are infinite and the perturbation increases exponentially. As a result, it is simple to demonstrate that modulation stability occurs when $L+M\neq 0$.

6. Results and discussion

Considering the double linear form of the generalized (3+1)-KP equation, which physically models the waves occurring in a medium, different exact solutions have been produced with a new technique consisting of the combination of the exponential and hyperbolic sine function. The new solutions of traveling wave produced for the GKP model are in the form of equation (21). In the model of this traveling wave, both exponential and hyperbolic form are designed as a combination. The Hirota binary linear form gives this wave design model greater significance. One of the generated traveling wave solutions can be chosen to elaborate the discussion about waves in a ferromagnetic medium. The traveling wave solution chosen without any criteria can play a key role in understanding nonlinear wave propagation. For the evolution equation discussed in this study, the findings will shed light on the nonlinear wave propagation mechanism through new mechanical structures and new properties. On the other hand, it can be said that the interaction between solitons for integrable models is flexible. The interaction between solitons in the KP equation, like many other integrable equations such as Sharma–Tasso–Olver model and the Burgers model, may not be entirely elastic [42]. If the circumstances are right, several solitons may merge or one soliton may divide into several solitons through the interaction of traveling waves. While the splitting of the solitons is referred to as the fission phenomena in the literature, the union of the solitons is referred to as the fusion phenomena [24]. In this study, it will shed light on the physical fission phenomenon and a simulation of the fission soliton formation will be included.

Let us employ equation (32) from the traveling wave solutions, which are the evolution equation's new mechanical structures. In equation (17), the variables m, k, n, a, b, c, d and v, which are mathematically arbitrary constants, have physical meanings as well. The wave frequencies are denoted by a, m, the number of waves are denoted by k, b, c and the wave speeds are represented by v, d [51]. The parameter a, which has a direct effect on the frequency, number and speed of the wave, will be used to further the discussion in this study. Other than a in equation (32), which is the subject of discussion, all other parameters are treated as constants. In the light of this information, we can present the following simulation for different values of a in equation (32).

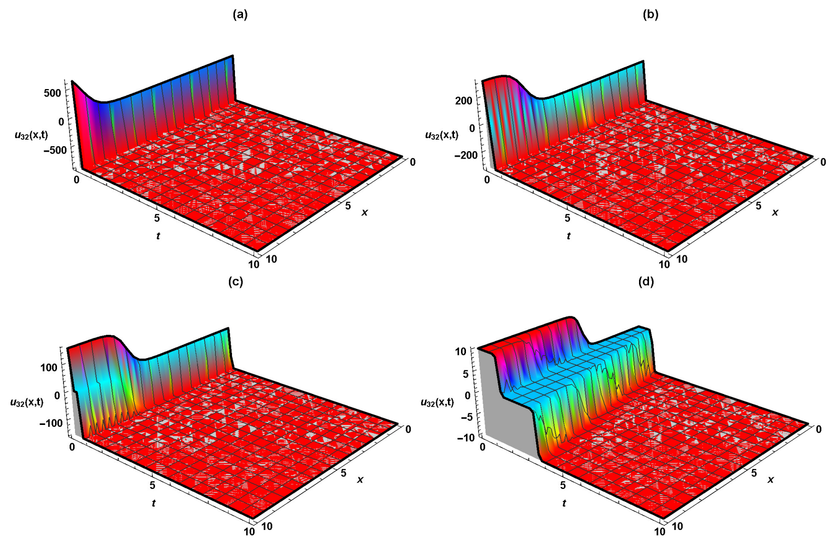

FIGURE 17. 3D graphs equation (32) for $b = 20,\ c = 2.3,\ d = 0.108,\ k = 0.03,\ \beta = 0.45,\ h_1 = 0.3,\ h_2 = 0.4,\ h_3 = 1.6,\ y = 1,\ z = 1$ and (a) for $a = 0.1$ (b) for $a = 0.15$ (c) for $a = 0.2$ (d) for $a = 0.6$.

The mathematical link between the frequency, number and velocity of the wave, as shown in equations (17) and (32), reveals the intricacy of physical dynamics. The response of different values of a, which plays an active role in the dynamics of nonlinear wave distribution and represents the number of waves physically, to the solution can be observed in Figure 17. The phenomenon of fusion of two solitary waves at a given moment without collision event can be clearly observed with the selected parameters. On the other hand, changes in x position without changing the solitary wave properties for different values of time parameter t can be observed in the graph below. It is clear from this

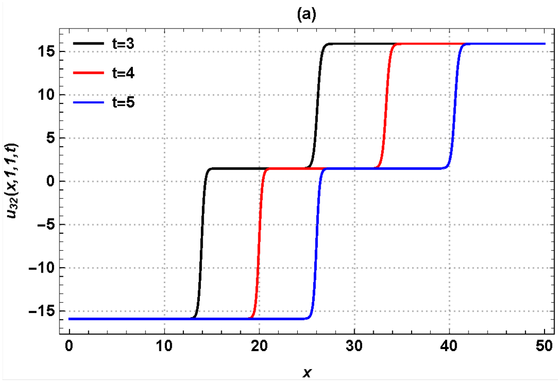

FIGURE 18. 2D graph of equation (32) for $a = 0.5,\ b = 20,\ c = 2.3,\ d = 0.108,\ k = 0.03,\ \beta = 0.45,\ h_1 = 0.3,\ h_2 = 0.4,\ h_3 = 1.6,\ y = 1,\ z = 1.$

analysis that the GKP equation is the only new traveling wave solution for the sole soliton that results from the union of two solitons. The fission phenomenon will be shed light on and we can conclude that the fission soliton formation is a traveling wave at different time values of t, as seen in Figure 18. Additionally, it can be seen that the advancing wave, whose direction of wave motion depends on the sign of the wave velocity, also moves to the right in the x's direction. The traveling solitary wave, which exhibits soliton properties without spoiling any of its properties, also contains the fusion phenomenon. As a result, this traveling wave deserves a nomination for a fusion soliton under the suitable conditions.

When equation (32) is thoroughly examined, it becomes clear that one of the key wave dynamics that impacts the traveling wave's frequency and speed is the parameter a, which stands for the wave number. Therefore, the velocity of the traveling wave, its response to the traveling wave solution for various values of a, can be analyzed. The figure below can be carefully scrutinized for this analysis.

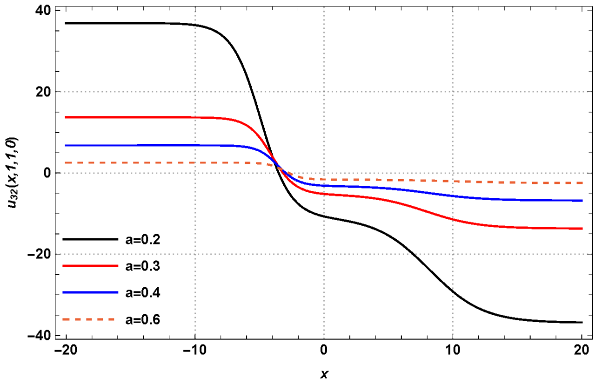

FIGURE 19. 2D graph of equation (32) for $b = 1,\ c = 2.3,\ d = -0.108,\ k = 0.03,\ \beta = 0.45,\ h_1 = 0.3,\ h_2 = 0.4,\ h_3 = 1.6,\ y = 1,\ z = 1,\ t = 0$.

Figure 19 was created with the intention of analyzing the impact of the a parameter, which is crucial to the dynamics of the traveling solitary wave on the velocity of the wave. The wave velocity corresponding to the $a = 0.2, a = 0.3, a = 0.4, a = 0.6$, value, respectively, is in the form of $1.549, 0.831, 0.529, 0.273$. As a increases, the wave velocity and amplitude decreases. In addition, it can be noticed that the propagating wave turns into a single soliton as its velocity decreases. The following three dimensional graphs make these inferences easier to see.

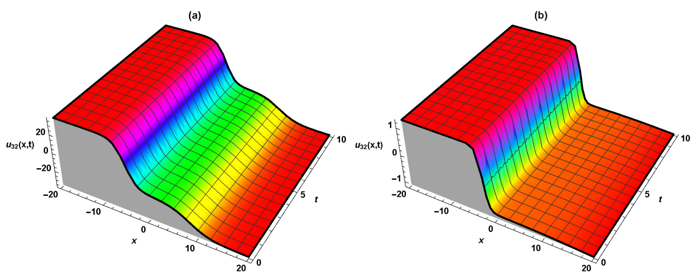

FIGURE 20. 3D graphs equation (32) for 2D graph of equation (32) for $b = 1,\ c = 2.3,\ d = -0.108,\ k = 0.03,\ \beta = 0.45,\ h_1 = 0.3,\ h_2 = 0.4,\ h_3 = 1.6,\ y = 1,\ z = 1,\ t = 0$. and (a) for $a = 0.2$ (b) for $a = 0.8$.

Solitons theory allows for many considerations of traveling wave solutions with complicated dynamics. Different suggestions for experimental researchers may be possible as a result of these scientific talks.

7. Conclusion

In this study, a new approximation technique consisting of the combination of the hyperbolic sine function and exponential function with the help of Hirota bilinear form for the generalized $(3+1)-$Kadomtsev-Petviashvili equation has been used. Through this new technique, many new solitary wave solutions of the nonlinear evolution model have been achieved. Graphics of these exact solutions, as seen in three dimensional, two dimensional and contour at any instant, the evolution of periodic properties are shown. Modulation instability has been used to search for the stability of the obtained solutions. Linear stability analysis technique has been used to evaluate the stability of the evolution equation. In addition, the fusion phenomenon is encountered in the equation (32) traveling wave solution analyzed for discussion. Fission soliton evolution have been simulated for different values of the wave number a, which play important roles in many dynamics of the traveling wave. The findings from this study open up new horizons for further exploration of the concept.

8. Author Contributions

M.A.I.: Methodology, Software, Conceptualization, Validation, Investigation, Writing - Original Draft, Visualization, Data Curation. A.Y.: Methodology, Conceptualization, Validation, Investigation, Writing - Original Draft, Writing - Review & Editing, Visualization, Supervision, Project Administration. All authors discussed the results and contributed to the final manuscript.

9. Data Availability Statement

The researchers claim that information confirming the study's findings is included in the publication and that the figures are actual expressions of that facts

10. Ethical considerations

The authors guarantee that this work complies with ethical norms.

11. Funding

This research received no specific grant from any funding agency in the public, commercial, or not-for-profit sectors.

12. Conflict of interest

The researchers affirm that they are free of any known financial conflicts of interest or close personal ties that might have looked to have affected the research presented in this study

References

[1] Akram, G., Sadaf, M., & Khan, M. A. U. (2022). Abundant optical solitons for Lakshmanan–Porsezian–Daniel model by the modified auxiliary equation method. Optik, 251, 168163.

[2] Aziz, K. H. A. N., Abbas, K. H. A. N., & Sinan, M. (2022). Ion temperature gradient modes driven soliton and shock by reduction perturbation method for electron-ion magneto-plasma. Mathematical Modelling and Numerical Simulation with Applications, 2(1), 1-12.

[3] Cui, P. (2021). Bilinear form and exact solutions for a new extended (2+ 1)-dimensional Boussinesq equation. Results in Physics, 22, 103919.

[4] Darwish, A., Ahmed, H. M., Ammar, M., Ali, M. H., & Arnous, A. H. (2022). General Solitons and other solutions for coupled system of nonlinear Schrödinger's equation in magneto-optic waveguides with anti-cubic law nonlinearity by using improved modified extended tanh-function method. Optik, 251, 168369.

[5] Duran, S. (2021). Breaking theory of solitary waves for the Riemann wave equation in fluid dynamics. International Journal of Modern Physics B, 35(09), 2150130.

[6] Duran, S., Yokuş, A., & Durur, H. (2021). Surface wave behavior and refraction simulation on the ocean for the fractional Ostrovsky–Benjamin–Bona–Mahony equation. Modern Physics Letters B, 35(31), 2150477.

[7] Eskandar, S., & Hoseini, S.M. (2017). Nearly solitons for a perturbed higher-order nonlinear Schrodinger equation. J. Mahani math. res. 6(1), pp.43-56.

[8] Ghanbari, B. (2021). Employing Hirota's bilinear form to find novel lump waves solutions to an important nonlinear model in fluid mechanics. Results in Physics, 29, 104689.

[9] Griffiths, G. W. (2012). Hirota Direct Method. City University, London.

[10] Hajiaghasi, S., & Azami, S. (2023). Gradient Ricci Bourguignon solitons on perfect fluid space-times. Journal of Mahani Mathematical Research, 1-12.

[11] He, J., Xu, S., & Porsezian, K. (2012). N-order bright and dark rogue waves in a resonant erbium-doped fiber system. Physical Review E, 86(6), 066603.

[12] Hu, W. Q., Gao, Y. T., Jia, S. L., Huang, Q. M., & Lan, Z. Z. (2016). Periodic wave, breather wave and travelling wave solutions of a (2+ 1)-dimensional B-type Kadomtsev-Petviashvili equation in fluids or plasmas. The European Physical Journal Plus, 131, 1-19.

[13] Isah, M. A. (2023). A novel technique to construct exact solutions for the Complex Ginzburg-Landau equation using quadratic-cubic nonlinearity law. Mathematics in Engineering, Science & Aerospace (MESA), 14(1).

[14] Isah, M. A., Isah, I., Hassan, T. L., & Usman, M. (2021). Some characterization of osculating curves according to darboux frame in three dimensional euclidean space. International Journal of Advanced Academic Research, 7(12), 47-56.

[15] Isah, M. A., & Kulahci, M. A. (2019). Involute Curves in 4-dimensional Galilean space G4. In Conference Proceedings of Science and Technology (Vol. 2, No. 2, pp. 134-141). Murat TOSUN.

[16] Isah, M. A., Yokus, A., & Kaya, D. (2024). Exploring the influence of layer and neuron configurations on Boussinesq equation solutions via a bilinear neural network framework. Nonlinear Dynamics, 1-17. https://doi.org/10.1007/s11071-024-09708-3

[17] Isah, M. A., Yokus, A., & Kaya, D. (2024). Bilinear neural network method for obtaining the exact analytical solutions to nonlinear evolution equations and its application to KdV equation. Khayyam Journal of Mathematics. Accepted paper.

[18] Isah, M. A., & Yokus, A. (2023). Optical solitons of the complex Ginzburg-Landau equation having dual power nonlinear form using φ^6-model expansion approach. Mathematical Modelling and Numerical Simulation with Applications, 3(3), 188-215.

[19] Isah, M. A., & Yokus, A. (2022). Application of the newly φ^6- model expansion approach to the nonlinear reaction-diffusion equation. Open Journal of Mathematical Sciences. 6, 269-280. doi:10.30538/oms2022.0192

[20] Isah, M. A., & Yokus, A. (2023). Rogue waves and stability analysis of the new (2+ 1)-KdV equation based on symbolic computation method via Hirota bilinear form. In 2023 International Conference on Fractional Differentiation and Its Applications (ICFDA) (pp. 1-6). IEEE.

[21] Isah, M. A., & Yokus, A. (2024). Nonlinear Dispersion Dynamics of Optical Solitons of Zoomeron Equation with New φ^6-Model Expansion Approach. Journal of Vibration Testing and System Dynamics, 8(03), 285-307.

[22] Isah, I., Isah, M. A., Baba, M. U., Hassan, T. L., & Kabir, K. D. (2021). On integrability of silver Riemannian structure. International Journal of Advanced Academic Research, 7(12), 2488-9849.

[23] Izadi, M., Yadav, S. K., & Methi, G. (2024). Two efficient numerical techniques for solutions of fractional shallow water equation. Partial Differential Equations in Applied Mathematics, 9, 100619.

[24] Jin-Ping, Y. (2001). Fission and fusion of solitons for the (1+ 1)-dimensional Kupershmidt equation. Communications in Theoretical Physics, 35(4), 405.

[25] Kaya, D., Yokuş, A., & Demiroğlu, U. (2020). Comparison of exact and numerical solutions for the Sharma–Tasso–Olver equation. Numerical solutions of realistic nonlinear phenomena, 53-65.

[26] Li, L., & Xie, Y. (2021). Rogue wave solutions of the generalized (3+ 1)-dimensional Kadomtsev–Petviashvili equation. Chaos, Solitons & Fractals, 147, 110935.

[27] Liu, J. G., Tian, Y., & Zeng, Z. F. (2017). New exact periodic solitary-wave solutions for the new (3+ 1)-dimensional generalized Kadomtsev-Petviashvili equation in multi-temperature electron plasmas. AIP Advances, 7(10).

[28] Ma, W. X., & Fan, E. (2011). Linear superposition principle applying to Hirota bilinear equations. Computers & Mathematics with Applications, 61(4), 950-959.

[29] Ma, W. X., & Zhu, Z. (2012). Solving the (3+ 1)-dimensional generalized KP and BKP equations by the multiple exp-function algorithm. Applied Mathematics and Computation, 218(24), 11871-11879.

[30] Mohammad, A. A., & Can, M. (1996). Painlevé analysis and symmetries of the Hirota–Satsuma equation. Journal of Nonlinear Mathematical Physics, 3(1-2), 152-155.

[31] Myint-U, T., & Debnath, L. (2007). Linear partial differential equations for scientists and engineers. Springer Science & Business Media.

[32] Rosenau, P. (2005). Communications-WHAT IS... a Compacton?. Notices of the American Mathematical Society, 52(7), 738-739.

[33] Rosenau, P. (1994). Nonlinear dispersion and compact structures. Physical Review Letters, 73(13), 1737.

[34] Rosenau, P., & Hyman, J. M. (1993). Compactons: solitons with finite wavelength. Physical Review Letters, 70(5), 564.

[35] Tarla, S., Ali, K. K., & Yusuf, A. (2023). Exploring new optical solutions for nonlinear Hamiltonian amplitude equation via two integration schemes. Physica Scripta, 98(9), 095218.

[36] Tarla, S., Ali, K. K., Yilmazer, R., & Yusuf, A. (2022). New behavior of tsunami and tidal oscillations for Long-and short-wave interaction systems. Modern Physics Letters B, 36(23), 2250116.

[37] Tarla, S., Ali, K. K., Yusuf, A., Yılmazer, R., & Alquran, M. (2022). New explicit wave profiles of kundu-mukherjee-naskar equation through jacobi elliptic function expansion method.

[38] Wazwaz, A. M. (2008). Multiple-front solutions for the Burgers–Kadomtsev–Petviashvili equation. Applied mathematics and computation, 200(1), 437-443.

[39] Wazwaz, A. M. (2012). Multiple-soliton solutions for a (3+ 1)-dimensional generalized KP equation. Communications in Nonlinear Science and Numerical Simulation, 17(2), 491-495.

[40] Wang, X. B., Tian, S. F., Yan, H., & Zhang, T. T. (2017). On the solitary waves, breather waves and rogue waves to a generalized (3+ 1)-dimensional Kadomtsev–Petviashvili equation. Computers & Mathematics with Applications, 74(3), 556-563.

[41] Wang, S. (2022). Novel multi-soliton solutions in (2+ 1)-dimensional PT-symmetric couplers with varying coefficients. Optik, 252, 168495.

[42] Wang, S., Tang, X. Y., Lou, S& . Y. (2004). Soliton fission and fusion: Burgers equation and Sharma–Tasso–Olver equation. Chaos, Solitons & Fractals, 21(1), 231-239.

[43] Weiss, J. (1985). Modified equations, rational solutions, and the Painlevé property for the Kadomtsev–Petviashvili and Hirota–Satsuma equations. Journal of mathematical physics, 26(9), 2174-2180.

[44] Yan, Z., & Konotop, V. V. (2009). Exact solutions to three-dimensional generalized nonlinear Schrödinger equations with varying potential and nonlinearities. Physical Review E, 80(3), 036607.

[45] Yang, Q., & Zhang, H. (2021). On the exact soliton solutions of fifth-order Korteweg-de Vries equation for surface gravity waves. Results in Physics, 26, 104424.

[46] Yokuş, A. (2021). Simulation of bright–dark soliton solutions of the Lonngren wave equation arising the model of transmission lines. Modern Physics Letters B, 35(32), 2150484.

[47] Yokuş, A., Durur, H., Abro, K. A., & Kaya, D. (2020). Role of Gilson–Pickering equation for the different types of soliton solutions: a nonlinear analysis. The European Physical Journal Plus, 135, 1-19.

[48] Yokuş, A., Durur, H., Duran, S., & Islam, M. T. (2022). Ample felicitous wave structures for fractional foam drainage equation modeling for fluid-flow mechanism. Computational and Applied Mathematics, 41(4), 174.

[49] Yokus, A., & Isah, M. A. (2023). Dynamical behaviors of different wave structures to the Korteweg–de Vries equation with the Hirota bilinear technique. Physica A: Statistical Mechanics and its Applications, 622, 128819.

[50] Yokus, A., & Isah, M. A. (2023). Stability analysis and soliton solutions of the nonlinear evolution equation by homoclinic technique based on Hirota bilinear form. In 2023 International Conference on Fractional Differentiation and Its Applications (ICFDA) (pp. 1-6). IEEE.

[51] Yokus, A., & Isah, M. A. (2022). Stability analysis and solutions of (2+ 1)-Kadomtsev–Petviashvili equation by homoclinic technique based on Hirota bilinear form. Nonlinear Dynamics, 109(4), 3029-3040.

[52] Zheng-De, D., Mu-Rong, J., Qing-Yun, D., & Shao-Lin, L. (2006). Homoclinic bifurcation for Boussinesq equation with even constraint. Chinese Physics Letters, 23(5), 1065.

[53] Zheng-De, D., Zhen-Jiang, L., & Dong-Long, L. (2008). Exact periodic solitary-wave solution for KdV equation. Chinese Physics Letters, 25(5), 1531.

[54] Zhang, Y., & Ma, W. X. (2015). Rational solutions to a KdV-like equation. Applied Mathematics and Computation, 256, 252-256.

Muhammad Abubakar Isah
Orcid number: 0000-0001-9129-5657
Department of Mathematics, Faculty of Science
Firat University
Elazig, Turkey
Email address: myphysics_09@hotmail.com

Asif Yokus
Orcid number: 0000-0001-7568-2251
Department of Mathematics, Faculty of Science
Firat University
Elazig, Turkey
Email address: asfyokus@firat.edu.com.tr